



This open access document is posted as a preprint in the Beilstein Archives at <https://doi.org/10.3762/bxiv.2020.98.v1> and is considered to be an early communication for feedback before peer review. Before citing this document, please check if a final, peer-reviewed version has been published.

This document is not formatted, has not undergone copyediting or typesetting, and may contain errors, unsubstantiated scientific claims or preliminary data.

Preprint Title Doxorubicin loaded gold nanorods: a multifunctional chemophotothermal nano-platform for cancer management

Authors Uzma A. Awan, Abida Raza, Shaukat Ali, Rida F. Saeed and Nosheen Akhtar

Publication Date 28 Aug 2020

Article Type Full Research Paper

ORCID® IDs Abida Raza - <https://orcid.org/0000-0002-4414-1070>; Shaukat Ali - <https://orcid.org/0000-0003-2481-1978>; Nosheen Akhtar - <https://orcid.org/0000-0003-3413-9150>

License and Terms: This document is copyright 2020 the Author(s); licensee Beilstein-Institut.

This is an open access publication under the terms of the Creative Commons Attribution License (<https://creativecommons.org/licenses/by/4.0>). Please note that the reuse, redistribution and reproduction in particular requires that the author(s) and source are credited.

The license is subject to the Beilstein Archives terms and conditions: <https://www.beilstein-archives.org/xiv/terms>.

The definitive version of this work can be found at <https://doi.org/10.3762/bxiv.2020.98.v1>

Doxorubicin loaded gold nanorods: a multifunctional chemo-photothermal nano-platform for cancer management

Uzma Azeem Awan^{1,2} Abida Raza^{2*}, Shaukat Ali³, Rida Fatima Saeed¹ Nosheen Akhtar¹

¹*Department of Biological Sciences, National University of Medical Sciences (NUMS), Rawalpindi, Pakistan*

²*NILOP Nanomedicine Research Laboratories, National Institute of Lasers and Optronics College, (PIEAS), Islamabad, Pakistan*

³*Medical Toxicology Lab, Department of Zoology, Government College University Lahore, Lahore-54000, Pakistan*

*Corresponding Authors:

Dr Abida Raza

Head NILOP Nanomedicine Research Laboratories

National Institute of Laser Optronics, Pakistan Institute of Engineering and Applied Sciences. Lehar road, Nilore, Islamabad, Pakistan

Tel +92519248671-6 ext 3103, 3177

Fax: +92 51 2208051

Email: abida_rao@yahoo.com

ORCID 0000-0002-4414-1070

Abstract

One of the limitations associated with cancer treatment is low efficacy and high dose-related side effects of anticancer drugs. The purpose of the current study was to fabricate biocompatible multifunctional drug loaded nano-moieties for co-therapy (chemo-photothermal therapy) with maximum efficiency and minimum side effects. Herein, we report *in vitro* anticancerous effects of doxorubicin (DOX) loaded on polyelectrolyte-poly (sodium-4-styrenesulfonate) coated Gold nanorods (PSS-GNRs) with and without NIR laser (808 nm, power density = 1.5 W/cm² for 2 min) exposure. Drug loading capacity of PSS-GNRs was about 76% with drug loading content of 3.2 mg DOX/mL. Cumulative DOX release significantly increased after laser exposure (1.5

W/cm²) compared to non-irradiated samples ($p < 0.05$). Zeta potential of GNRs, PSS-GNRs and DOX-PSS-GNRs was recorded as $+42 \pm 0.1$ mV, -40 ± 0.3 mV and 39.3 ± 0.6 mV, respectively. PSS-GNRs nano-complexes were found biocompatible and showed higher photothermal stability. DOX conjugated nano-complexes with NIR laser irradiation appear more efficient in cell inhibition (93%) than without laser exposure (65%) and doxorubicin alone (84%). The IC₅₀ of PSS-GNRs-DOX and PSS-GNRs-DOX was recorded as 7.99 ± 0.0032 and 3.12 ± 0.0906 $\mu\text{g/mL}$ with laser irradiation. Thus, a combinatorial approach based on chemo and photothermal strategy appears to be a promising platform in cancer management.

Keywords

Chemotherapy; Doxorubicin; Gold nanorods; NIR laser; Photothermal therapy

Introduction

Regardless of enormous advances in medical research, cancer is still the second leading cause of death worldwide and has killed 8.8 million peoples in 2015 [1]. Currently, there are number of treatment modalities, including chemotherapy, immunotherapy, targeted therapy, radiations, and surgery [2]. Among these, chemotherapy is the most commonly used method for treatment of various cancers [3]. However, use of conventional chemotherapeutic agents in cancer treatment is limited, due to several unwanted characteristics of poor solubility, broad bioavailability range, narrow therapeutic index, rapid elimination from systemic circulation, unselective site of action after oral/intravenous administration, and cytotoxic effects on normal tissues [4]. Such problems can be overcome by advanced drug delivery systems which offer carrier systems to hold sufficient amount of drug, with prolonged circulation time sustained drug release within tumor tissues and distinctive accumulation behavior at the tumor site [5]. Nanocarriers can improve

pharmacological properties of free drugs that contribute towards enhanced therapeutic efficacy in physiological environment [6].

Designing of multi-functional tumor targeting and therapeutic agent nanocarriers, provides a multimodal and effective approach such as significant absorption or scattering in the visible and near-infrared (NIR) regions, tunable aspect ratio, biocompatibility, fluorescence properties and ease of biofunctionalization make them ideal nanocarriers in biomedical applications [8]. Cetyl Trimethyl Ammonium Bromide (CTAB) is indispensable for synthesizing particles to direct the growth and stabilize the shape of gold nanorods but CTAB coated GNRs cannot be used in applications with the cells because of their high cytotoxicity [9]. Different polymers can be used to coat GNRs, to enhance their biocompatibility and dispersion at physiological pH. The positive CTAB layer on GNRs surface facilitates electrostatic adsorption of anionic compounds such as polysodium 4-styrenesulfonate (PSS) which ultimately facilitate electrostatic interaction with cationic anticancerous drugs like doxorubicin (DOX) [10, 11]. DOX, an anticancer drug is extensively used in the management of different tumors [12]. Antitumor activity of the drug is exerted by interaction with DNA replication [13]. High dose regimens of DOX are associated with severe cardiotoxicity and bone marrow suppression. Different strategies are being used to encapsulate the drug to minimize its side effects; however this decreased the chemotherapeutic effectiveness [14]. To address these issues, advanced synergistic therapies such as combination of chemotherapy and photothermal therapy have been applied to enhance the overall therapeutic efficacy. This includes gold nanorods capped magnetic core, silica nanorattle gold shells and DNA based platform loaded with GNRs and DOX [15-17].

In the current study, DOX conjugated with PSS coated GNRs are designed for photothermal therapy. We hypothesized that our designed multimodal system will ruin tumor cells after NIR exposure (808 nm) via hyperthermia induced apoptosis and necrosis.

Results and Discussion

DOX loaded GNRs nano-complex fabrication

The prepared GNRs suspension has a surplus of cytotoxic CTAB, which was removed by repetitive cycles of centrifugation and re-dispersion. A CTAB bilayer remained non-covalently conjugated onto the GNRs surface to maintain the stability of the final product. The longitudinal localized plasmon resonance (LSPR) and the transverse plasmon resonance (TSPR) of prepared GNRs was found to be 780 and 526 nm, respectively (Figure 1a). TEM images display mono-dispersed rods with aspect ratio 4.2 (Figure 1b & 1c). The biocompatible GNRs were prepared by PSS coating on their surface. The LSPR peak of the PSS coated GNRs was slightly red shifted to 783 nm (Figure 1c). The shift in LSPR peak after PSS coating is due to the side by side assembly of the PSS-GNRs.

Absorption spectra confirmed the successful loading of chemotherapeutic drug (DOX) on PSS coated GNRs (Figure 1d). The polyelectrolyte coating allowed GNRs to easily interact with the surrounding environment, consequently the wavelength of LSPR of GNRs perceptively responded to the refractive index change caused by molecular adsorption. The conjugation of DOX onto the PSS-GNRs surface resulted in red shift of the LSPR band, while the TSPR peak remained same. Increased local refractive index around GNRs due to adsorption of DOX might lead to stronger the Columbic restoring force and red shift of the LSPR peak [18]. The percentage yield of the DOX-PSS-GNRs was found to be $81.2\% \pm 0.21$. To confirm the surface chemistry modification of GNRs the zeta-potential of CTAB-GNRs, PSS-GNRs and DOX-PSS-

GNRs were investigated. The zeta potential of unrefined GNRs was measured to be $+60 \pm 0.2$ mV which decreased to $+42 \pm 0.1$ mV after removal of excess CTAB (two rounds of centrifugation and re-dispersion). A negative zeta-potential of -40 ± 0.3 mV was recorded after successful coating of PSS on GNRs surface and again positive (39.3 ± 0.6 mV) of DOX-PSS-GNRs confirmed chemistry changes to the GNRs surface (Figure 1e).

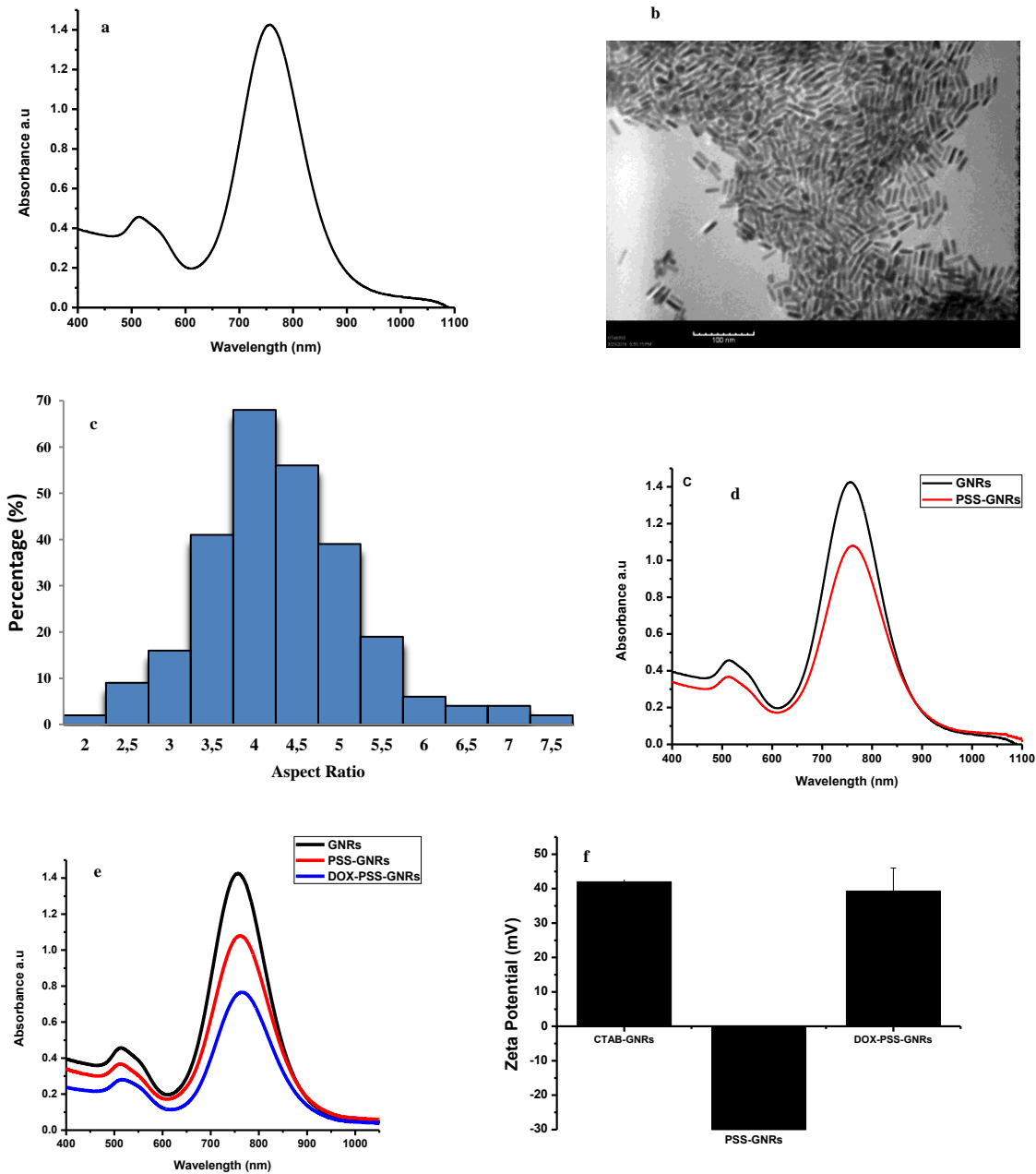


Figure 1: (a) UV–Vis absorption spectrum of bare GNRs illustrated peak absorption intensity at 780 nm (b) TEM image shows monodispersed GNRs having 4.2 aspect ratio. (c) Histogram showing GNRs aspect ratio (d) PSS coating of GNRs causes a red shift in the LSPR peak. (e) A further red shift in LSPR peak absorption intensity was recorded with DOX loading on the PSS-GNRs. (f) Zeta-Potential (mV) for CTAB coated GNR, PSS-GNRs and DOX-PSS-GNRs. The CTAB-GNRs have a positive charge after synthesis, a negative zeta-potential after PSS coating and again positive potential after conjugating with DOX (Final product of DOX-PSS-GNRs). Each bar represents the mean value \pm SEM of triplicates.

Drug loading efficiency (DLE)

The loading efficacy of DOX on the PSS-GNRs was measured systematically using a standard curve of absorption of DOX (at 490 nm) by changing the concentration of DOX against the fixed concentration of PSS-GNRs (40 μ g/mL). Molar absorptivity was recorded to be 0.87. Drug loading capacity of PSS-GNRs was about 76% with drug loading content of 3.2 mg DOX/mL of GNRs.

Photothermal stability of PSS-GNRs

Optical characterization of PSS-GNRs showed the LSPR peak of GNRs strongly depends on their aspect ratio, therefore, the LSPR peak position is an excellent indicator for any shape changes of GNRs. Aqueous solution of PSS-GNRs after laser exposure for 2 min (power density = 1.5 W/cm²) remain stable, the LSPR peak shifted approximately 4 nm (Figure 2). Stability of PSS-GNRs after NIR laser exposure was good enough for photothermal therapy.

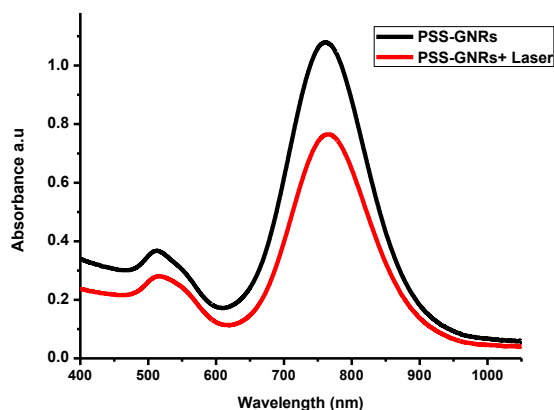


Figure 2: PSS-GNRs before and after 808 nm laser exposure, the LSPR peak was a shifted about 4 nm.

***In vitro* DOX release after NIR exposure**

Drug release from PSS-GNRs can easily be controlled with NIR irradiation. The cumulative DOX release almost doubled after laser exposure (1.5 W/cm^2) compared to non-irradiated samples (Figure 3). Enhanced drug release stimulated by laser (808 nm) may possibly because of the heat generated by the nanomaterial. DOX release from irradiated samples was significantly reduced after 5 hrs as extracellular tissues of tumors and intracellular lysosomes have acidic environment (pH 5-6), so DOX release experiment was conducted at 5.6 pH [19].

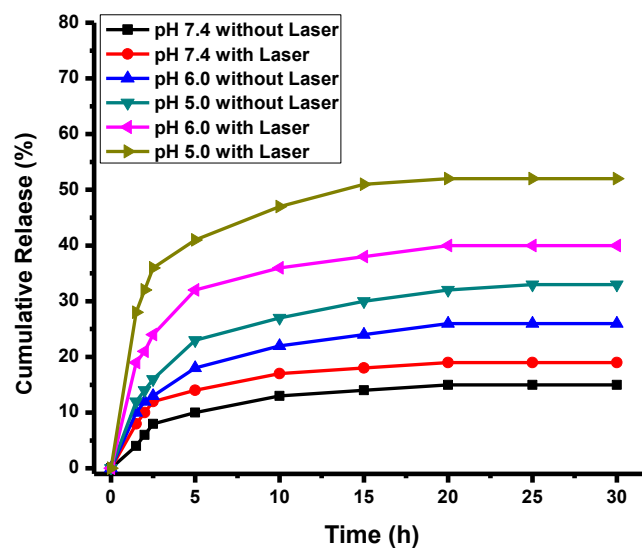


Figure 3: *In vitro* DOX release profile from PSS-GNRs: NIR-triggered DOX release at various pH. DOX-PSS-GNRs solutions were irradiated with CW NIR laser (808 nm, 1.5 W/cm²) for 2 min and fluorescence intensity was recorded after 1, 2, 3, 4 and 5 h.

PSS-GNRs nano complex biocompatibility

Dose dependent biocompatibility and cytotoxicity efficiency of the nanocarriers was recorded *in vitro*. The efficiency of the GNRs in mediating cytotoxicity against HepG2 (carcinogenic) and 3T3 (non-carcinogenic) cells was evaluated. Cells were treated for 12 h with PSS-GNR and analyzed using the MTT assay. Figure 4 showed that exposure of cells with PSS-GNR had no significant reduction in the cells viability compared to control cells as viability remained higher than 88%, at the concentration of 500 µg/mL for HepG2 cells and 1000 µg/mL for 3T3 cells (Figure 4a). If nanoparticles interact with RBCs in the blood stream they can cause hemolysis. Therefore hemolytic properties and interaction with RBCs are the main parameters for the biocompatibility of nanocarriers [19]. Analysis of hemoglobin released from RBCs after incu-

bation in a suspension of PSS-GNRs showed less than 20% hemolysis at the concentration of 1000 $\mu\text{g/mL}$ (Figure 4b). The testing experiments revealed good biocompatibility for PSS-GNRs nano-carrier as quantified by the concentration of hemoglobin in the supernatant of GNRs-RBCs mixture by monitoring absorbance intensity at 570 nm. The absence of marked haemotoxicity for this sample is mainly related to the presence of polymer, as GNRs surface had no direct contact with the RBCs because of completely passivated by PSS coating.

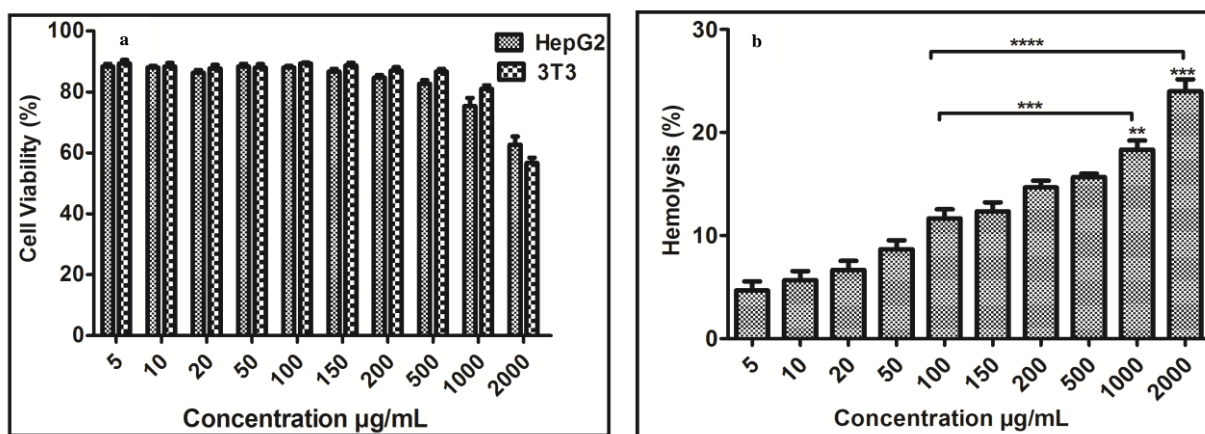


Figure 4: (a) HepG2 and 3T3 cells relative viabilities after being incubated at the different concentrations of PSS-GNRs for 24 h. (b) Haemotoxicity assay on PSS-GNRs shows PSS-GNRs are hemo-compatible. No significant difference was seen from 5-500 $\mu\text{g/mL}$ (<20% hemolysis). Low significant (***) and high significant difference (****) was seen in case of 1000 and 2000 $\mu\text{g/mL}$ when compared with 100 $\mu\text{g/mL}$. Each bar shows the mean value \pm SEM of triplicates.

Cell Inhibition after NIR exposure of PSS-GNR-DOX complexes

Optically triggered drug release from PSS-GNR-DOX by NIR laser (808 nm) exposure at an output power density of 1.5 W/cm^2 on HepG2 cells was studied. DOX release from PSS-GNR-DOX was increased significantly ($p < 0.05$) after 2 min of NIR irradiation (Figure 5). HepG2 cells were treated with free DOX and DOX-PSS-GNRs, either irradiated with NIR laser or not exposed to NIR light. Dose-dependent cytotoxicity was observed in all study groups. About 84%

of cells were killed by free DOX and 65% by DOX-PSS-GNRs at equivalent DOX concentration of 10 $\mu\text{g/mL}$ (Figure 5). This showed that, free DOX was more toxic as compared to DOX conjugated to a nano-carrier at the same drug concentration. Similar findings were reported by Zhang and coworkers [20]. The high cytotoxic effect might exhibited by free DOX is due to higher availability of drug to the cells after the cell uptake whereas; the decreased cytotoxicity with DOX-PSS-GNRs is because of delayed drug release inside cells [19]. PSSGNRs nano-complex has promising potential as biocompatible nanocarriers for drug loading and delivery in cancer therapy. Previous report showed DOX loaded tiopronin coated gold nanoparticles (Au-TIOP-DOX) had a better effect in killing cancer cells than free DOX [21]. The cytotoxic efficiency of the DOX-loaded PAA-PEG-GNRs was found to be similar to free DOX and improved with an increase in their concentrations [10]. In a previous study GNR-DOX-cRGD, viability was significantly decreased down to 57%, whereas free DOX demonstrated the highest level of cytotoxicity (41% of control) in U87MG cells [22]. We found that DOX-PSS-GNRs complexes killed more cancer cells (93%) after NIR laser irradiation (Figure 5). Higher cytotoxicity of complex is due to the enhanced release of drug upon NIR laser irradiation. The IC_{50} of complex (PSS-GNRs-DOX) was $7.99 \pm 0.0032 \mu\text{g/mL}$ and for PSS-GNRs-DOX with laser irradiation was $3.12 \pm 0.0906 \mu\text{g/mL}$. The IC_{50} of free DOX and DOX with laser exposure was 3.999 ± 0.04211 and $4.41 \pm 0.0037 \mu\text{g/mL}$, respectively. Previously, Au-HNS-EGFR-DOX are reported to have significant antiproliferative activity against lung cancer cells when irradiated with NIR laser (125 mW/cm^2 , 25 s) in contrast to non-exposed cells [23]. Free DOX showed no significant change on viability, for both with and without laser. This indicates that increased cell death upon NIR laser irradiation might be attributed to the presence of gold nano-carrier. Without laser treatment low drug release was observed from nano-complex, showing that drug

release was turned off without laser illumination. Laser (808 nm) triggered DOX release was recorded using the same laser treatment at different time intervals (2, 3, and 4 hrs) in which drug release was improved in time dependent fashion. Below 10% of DOX was released within 4 h from PSS-GNR-DOX without NIR exposure, using the same experimental conditions (Figure 5). Drug release from the nano-complex (PSS-GNR-DOX) might be easily turned “on” and “off” by NIR laser exposure. The NIR laser irradiation cause melting of PSS that would lead to decreased stability and enhanced drug diffusion coefficient. No drastic change was observed in temperature of the solution after NIR irradiation. Mild NIR irradiation might cause a rapid and localized raised in the temperature on the GNRs surface, which leads to melt the PSS coating and accelerate drug release. Our study suggests that co-therapy based on combined chemo and photothermal treatment using nano-carriers is a best choice for cancer management. Low dosage treatment minimize side effect and maximize therapeutic efficiency of drug [19].

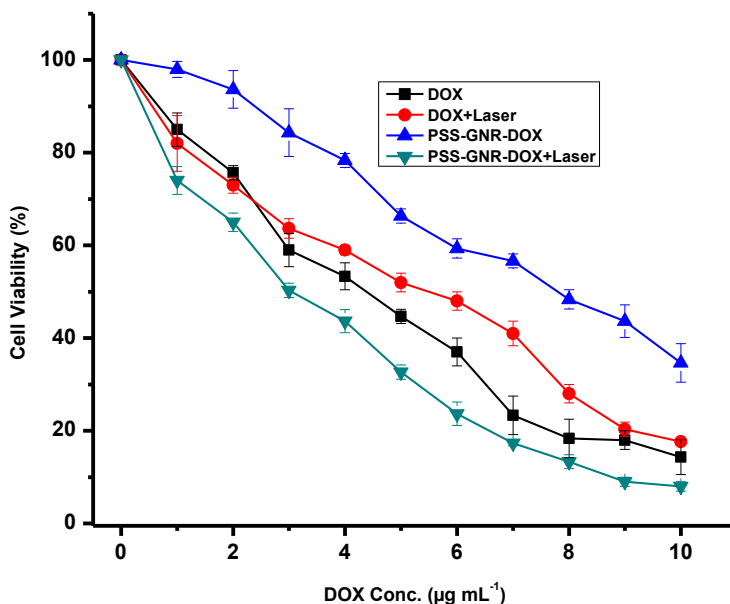


Figure 5. Percentage viabilities of HepG2 cells treated with free DOX and DOX-PSS-GNRs exposed to NIR light (1.5 W/cm^2 for 2 min per treatment, three treatments over 2 h). The cytotoxicity with and without laser have significant difference with $p < 0.05$ in case of DOX-PSS-GNRs by two-sample student *t*-test.

Conclusion

Successful loading of DOX onto PSS-GNRs have been demonstrated in the current study. The nano-platform, we proposed, showed high biocompatibility *in vitro* cell studies and were found photo-thermally stable. Higher cytotoxicity was observed with DOX-PSS-GNRs followed by NIR laser irradiation in contrast to DOX alone. PSS-GNRs-DOX nano-complexes are better than chemotherapy and photothermal therapy alone. Chemo-photothermal treatment based nano-complex system is a cost effective approach for reducing the high dose related side effects with enhanced therapeutic efficiency in cancer management.

Experimental Section

Materials

CTAB (H6269), hydrogen tetrachloroaurate (III) trihydrate ($\text{HAuCl}_4 \cdot 3\text{H}_2\text{O}$, 520918), L-ascorbic acid ($\text{C}_6\text{H}_8\text{O}_6$, 2555564), sodium borohydride (NaBH_4 , 452173), silver nitrate (AgNO_3 , 209139), Doxorubicin (D1515) poly (sodium 4-styrenesulphonate) (PSS; Mw 70,000) and 3-(4,5-dimethylthiazol-2-yl)-2, 5-diphenyltetrazolium bromide (MTT) were purchased from Sigma Aldrich. Deionized (DI) water, having resistance of $18 \text{ M}\Omega \text{ cm}$, was used throughout the experiments.

Gold nanorods synthesis

GNRs were synthesized through seed-mediated growth method with slight modification [24]. Gold seed particles were synthesized by adding 250 μL of 10 mM $\text{HAuCl}_4 \cdot 3\text{H}_2\text{O}$ to 10 mL of 0.1 M CTAB with continuous stirring. Freshly prepared, ice-cold 600 μL NaBH_4 solution (10 mM) was added followed by 30 min continuous stirring. For GNRs growth solution, 50 mL of 0.1 M CTAB was added to 2.5 mL of 10 mM $\text{HAuCl}_4 \cdot 3\text{H}_2\text{O}$. To the stirring solution 400 μL HCl (1 M), 500 μL AgNO_3 (10 mM) and 400 μL L-ascorbic acid (10 mM) was added. Finally, 200 μL of seed solution was added to the growth solution. GNRs were purified by centrifugation (14,000 g for 20 min) after 24 h of incubation. Then, the collected pellet was re-dispersed in deionized water.

PSS coating of GNRs

A reported method by Venkatesan was used, with slight modification, for PSS coating on GNRs [25]. Prepared GNRs (2 mL, 40 $\mu\text{g}/\text{mL}$) were centrifuged at 12000 g for 10 min and the pellet was re-dispersed in 2 mL of deionized water. GNRs solution was added drop-wise to 2 mL of PSS (2 mg/mL in 8 mM NaCl). For maximum adsorption, the solution was kept on stirring at room temperature for 2 h. Excess polymer (supernatant fraction) was removed by centrifugation (12000g for 10 min). PSS-stabilized GNRs were re-suspended in 2 mL deionized water and stored at 4°C.

Doxorubicin loaded PSS-GNRs

PSS-GNRs (40 $\mu\text{g}/\text{mL}$, 2 mL) were added to an aqueous solution of DOX at a final concentration of 10 $\mu\text{g}/\text{mL}$ and was stirred overnight in the dark at room temperature. Excess drug was removed by centrifugation at 12,000g for 10 min and pellet was re-dispersed in 2 mL deionized water. UV-Vis spectra of DOX loaded GNRs were scanned at a wavelength range of

400-1100 nm. Surface charge distribution of DOX loaded PSS-GNRs conjugate, at a different level, was determined by the zeta potential analyzer (Zetasizer Nano ZS90 DLS system Malvern Instruments Ltd., England).

Percentage yield

Nanoparticles were collected and weighed accurately. The percentage (%) yield was then calculated using formula given below [26]

$$\% \text{ yield} = \frac{\text{Mass of nanoparticles obtained}}{\text{Total weight of drug and polymer}} \times 100$$

Drug loading efficiency (DLE)

In order to calculate the drug loading efficiency, a known quantity of DOX was mixed with an aqueous PSS-GNRs solution (40 mg/mL) to get final drug concentration of 5, 10, 15, 20, 25, 50, 100, 200 and 300 mg/mL. Then the suspension was stirred overnight in the dark at 20°C. The suspension was then centrifuged at 12,000g for 10 min in order to precipitate the DOX-PSS-GNRs nano-conjugate and then dialyzed against pure water to remove the unbound DOX. The quantity of loaded DOX was recorded at 485 nm. Drug loading efficiency (DLE) was calculated using the formula given below.

$$\text{DLE (\%)} = \frac{\text{Amount of drug loaded} - \text{Free drug in supernatant}}{\text{Amount of drug loaded}} \times 100$$

Photothermal stability of PSS-GNRs

The photothermal stability of PSS-GNRs was recorded by irradiating conjugate with NIR laser (power density= 1.5 W/cm²) for 2 min. After laser treatment stability of the sample was analyzed by UV-Vis spectroscopy.

***In vitro* drug release by NIR exposure**

Near infrared (NIR) triggered drug release from PSS-GNRs was recorded in 10 mM phosphate buffer saline (PBS) (pH 5.6 at 37°C). A continuous wave 808 nm NIR laser (Ti-Sapphire, Spectra Physics CA 95054, USA) was used. DOX-PSS-GNRs (40 µg/mL, 2 mL) were dispersed in 10 mL of PBS followed by NIR laser irradiated at an output power of 1.5 W/cm² for 2 min and 800 µL of the resulting solutions was taken out for analysis. Exposed media was centrifuged at 12,000g for 10 min. Amount of DOX released from PSS-GNRs in the supernatant was determined by fluorescence measurement (Biotek synergy H4 multi-mode plate reader).

***In vitro* cytotoxicity assays**

The *in vitro* cytotoxicity of PSS-GNRs was recorded using 3T3 and HepG2 cells. Cells were seeded in 96 well plates (4x10³ cells per well). After 24 h of incubation, cells were exposed to different concentrations of PSS coated GNRs. Cells were allowed to incubate at 37°C for an additional 24 h. Viability was recorded by the MTT assay [27].

Hemolysis Assay

All human blood samples in this study were from healthy volunteers and used with Institutional Review Board (IRB) bioethics approval. The hemolysis assay was carried out according to the protocol from National Cancer Institute (NCI).

Whole blood (5 ml) from two healthy human donors was drawn directly into K2-EDTA-coated tubes to prevent coagulation. Blood collection was performed by a trained phlebotomist in order to minimize the risk to the donor. A written informed consent was obtained from each donor prior to the blood drawn.

In the 5 mL of blood 15 mL of sterilized phosphate buffer saline (PBS) was added and after slow agitation tubes were centrifuged at 500×g for 10 min. Supernatant containing plasma was aspirated and the buffy coat was washed thrice and diluted with normal saline to a 50% packed

cell volume (hematocrit) adjusted at pH 7.4 and stored at 4°C. Different concentrations of PSS-GNRs (100 µL each) were incubated with 100 µL of RBCs suspension at 37°C in CO₂ incubator for 4 h. 0.2% Triton ×100 was used as positive control and PBS was taken as negative control [28]. After incubation, 50 µL of 2.5% glutaraldehyde was added to the sample in order to stop the process of haemolysis and centrifuged at 1000×g for 10 min. Hemoglobin release was monitored at 562 nm using a microplate reader (Platos R496, Austria) by transferring supernatant to 96 well plate. Percentage hemolysis was recorded using following formula

$$\text{Percent Hemolysis} = \frac{\text{Sample absorbance} - \text{negative control absorbance}}{\text{Positive control absorbance} - \text{negative control absorbance}} \times 100$$

Cell Inhibition after Photothermal Treatment

The HepG2 cells were seeded into 96-well plates (5×10³ per well) and incubated for 24 h before the adding the different concentrations of PSS-GNRs, free DOX and PSS-GNRs-DOX conjugate. The treated cells were incubated for 12 h for proper uptake before laser irradiation. After that cells were illuminated by 808 nm NIR laser (power density =1.5 W/cm² for 2 min) and incubated at 37°C for 24 h. The MTT assay was performed to record cell inhibition.

Funding

The authors are thankful to Higher Education Commission, Pakistan (SRGP (NO.21-2219/SRGP/R&D/HEC/2018)) for financial support. We are grateful to Pakistan Science Foundation Islamabad, Pakistan, for financial assistance (PSF/Res/C-NILOP/Med (330)).

Conflict of Interest

The authors have no competing interests to declare.

References

1. World Health Organization. Cancer Fact sheet. Available from: <http://www.who.int/mediacentre/factsheets/fs297/en/> [last accessed on 16 May, 2019].
2. Feng, S.-S.; Chien, S., Chemotherapeutic engineering: application and further development of chemical engineering principles for chemotherapy of cancer and other diseases. *Chem. Eng. Sci.* **2003**, *58* (18), 4087-4114.
3. Lu, Y.-J.; Lin, P.-Y.; Huang, P.-H.; Kuo, C.-Y.; Shalumon, K.; Chen, M.-Y.; Chen, J.-P., Magnetic Graphene Oxide for Dual Targeted Delivery of Doxorubicin and Photothermal Therapy. *Nanomater.* **2018**, *8* (4), 193.
4. Ghaz-Jahani, M. A.; Abbaspour-Aghdam, F.; Anarjan, N.; Berenjian, A.; Jafarizadeh-Malmiri, H., Application of chitosan-based nanocarriers in tumor-targeted drug delivery. *Mol. Biotechnol.* **2015**, *57* (3), 201-218.
5. Lu, Y.-J.; Wei, K.-C.; Ma, C.-C. M.; Yang, S.-Y.; Chen, J.-P., Dual targeted delivery of doxorubicin to cancer cells using folate-conjugated magnetic multi-walled carbon nanotubes. *Colloids and Surfaces B.* **2012**, *89*, 1-9.
6. Farrell, D.; Alper, J.; Ptak, K.; Panaro, N. J.; Grodzinski, P.; Barker, A. D., Recent advances from the national cancer institute alliance for nanotechnology in cancer. *ACS. Nano.* **2010**, *4* (2), 589-594.
7. Yu, M. K.; Park, J.; Jon, S., Targeting strategies for multifunctional nanoparticles in cancer imaging and therapy. *Theranostics.* **2012**, *2* (1), 3.
8. Chakravarthy, K. V.; Bonoiu, A. C.; Davis, W. G.; Ranjan, P.; Ding, H.; Hu, R.; Bowzard, J. B.; Bergey, E. J.; Katz, J. M.; Knight, P. R., Gold nanorod delivery of an ssRNA immune activator inhibits pandemic H1N1 influenza viral replication. *Proc. Natl. Acad. Sci.* **2010**, *107* (22), 10172-10177.
9. Rayavarapu, R. G.; Petersen, W.; Hartsuiker, L.; Chin, P.; Janssen, H.; van Leeuwen, F. W.; Otto, C.; Manohar, S.; van Leeuwen, T. G., In vitro toxicity studies of polymer-coated gold nanorods. *Nanotechnology.* **2010**, *21* (14), 145101.
10. Wang, T.; Zhang, X.; Pan, Y.; Miao, X.; Su, Z.; Wang, C.; Li, X., Fabrication of doxorubicin functionalized gold nanorod probes for combined cancer imaging and drug delivery. *Dalton Trans.* **2011**, *40* (38), 9789-9794.
11. Gibson, J. D.; Khanal, B. P.; Zubarev, E. R., Paclitaxel-functionalized gold nanoparticles. *J. Am. Chem. Soc.* **2007**, *129* (37), 11653-11661.
12. Eliasson, C.; Lorén, A.; Murty, K.; Josefson, M.; Käll, M.; Abrahamsson, J.; Abrahamsson, K., Multivariate evaluation of doxorubicin surface-enhanced Raman spectra. *Spectrochim. Acta. A.* **2001**, *57* (9), 1907-1915.
13. Aryal, S.; Grailer, J. J.; Pilla, S.; Steeber, D. A.; Gong, S., Doxorubicin conjugated gold nanoparticles as water-soluble and pH-responsive anticancer drug nanocarriers. *J. Mater. Chem.* **2009**, *19* (42), 7879-7884.
14. Upadhyay, K. K.; Bhatt, A. N.; Mishra, A. K.; Dwarakanath, B. S.; Jain, S.; Schatz, C.; Le Meins, J.-F.; Farooque, A.; Chandraiah, G.; Jain, A. K., The intracellular drug delivery and anti tumor activity of doxorubicin loaded poly (γ -benzyl L-glutamate)-b-hyaluronan polymersomes. *Biomaterials.* **2010**, *31* (10), 2882-2892.
15. Ma, M.; Chen, H.; Chen, Y.; Wang, X.; Chen, F.; Cui, X.; Shi, J., Au capped magnetic core/mesoporous silica shell nanoparticles for combined photothermo-/chemo-therapy and multimodal imaging. *Biomaterials.* **2012**, *33* (3), 989-998.
16. Liu, H.; Chen, D.; Li, L.; Liu, T.; Tan, L.; Wu, X.; Tang, F., Multifunctional gold nanoshells on silica nanorattles: a platform for the combination of photothermal therapy and chemotherapy with low systemic toxicity. *Ange. Chem. Int.* **2011**, *123* (4), 921-925.
17. Xiao, Z.; Ji, C.; Shi, J.; Pridgen, E. M.; Frieder, J.; Wu, J.; Farokhzad, O. C., DNA Self-Assembly of Targeted Near-Infrared-Responsive Gold Nanoparticles for Cancer Thermo-Chemotherapy. *Ange. Chem. Int.* **2012**, *124* (47), 12023-12027.

18. Chen, H.; Ming, T.; Zhao, L.; Wang, F.; Sun, L.-D.; Wang, J.; Yan, C.-H., Plasmon–molecule interactions. *Nano Today*. **2010**, *5* (5), 494-505.
19. Liao, J.; Li, W.; Peng, J.; Yang, Q.; Li, H.; Wei, Y.; Zhang, X.; Qian, Z., Combined cancer photothermal-chemotherapy based on doxorubicin/gold nanorod-loaded polymersomes. *Theranostics*. **2015**, *5* (4), 345.
20. Zhang, Z.; Wang, J.; Nie, X.; Wen, T.; Ji, Y.; Wu, X.; Zhao, Y.; Chen, C., Near infrared laser-induced targeted cancer therapy using thermoresponsive polymer encapsulated gold nanorods. *J. Am. Chem. Soc.* **2014**, *136* (20), 7317-7326.
21. Huo, S.; Jin, S.; Zheng, K.; He, S.; Wang, D.; Liang, X., Preparation and characterization of doxorubicin functionalized tiopronin-capped gold nanorods for cancer therapy. *Chinese Sci. Bull.* **2013**, *58* (33), 4072-4076.
22. Xiao, Y.; Hong, H.; Matson, V. Z.; Javadi, A.; Xu, W.; Yang, Y.; Zhang, Y.; Engle, J. W.; Nickles, R. J.; Cai, W., Gold nanorods conjugated with doxorubicin and cRGD for combined anticancer drug delivery and PET imaging. *Theranostics*. **2012**, *2* (8), 757.
23. Noh, M. S.; Lee, S.; Kang, H.; Yang, J. K.; Lee, H.; Hwang, D.; Lee, J. W.; Jeong, S.; Jang, Y.; Jun, B. H.; Jeong, D. H.; Kim, S. K.; Lee, Y. S.; Cho, M. H., Target-specific near-IR induced drug release and photothermal therapy with accumulated Au/Ag hollow nanoshells on pulmonary cancer cell membranes. *Biomaterials*. **2015**, *45*, 81-92.
24. Awan, U. A.; Ali, S.; Rehman, M.; Zia, N.; Naz, S. S.; Ovais, M.; Raza, A. Stable and reproducible synthesis of gold nanorods for biomedical applications: a comprehensive study. *IET Nanobiotechnol.* **2018**, *12*(2), 182-190.
25. Venkatesan, R.; Pichaimani, A.; Hari, K.; Balasubramanian, P. K.; Kulandaivel, J.; Premkumar, K., Doxorubicin conjugated gold nanorods: a sustained drug delivery carrier for improved anticancer therapy. *J. Mater. Chem. B*. **2013**, *1* (7), 1010-1018.
26. Ankarao, A.; Naik, V.; Rao, K. H., Formulation and in vitro evaluation of oral sustained release nanoparticulate delivery system of carvedilol. *J. Pharm. Biomed. Sci.* **2012**, *3* (2), 924-928.
27. Denizot, F.; Lang, R., Rapid colorimetric assay for cell growth and survival. Modifications to the tetrazolium dye procedure giving improved sensitivity and reliability. *J. Immunol. Methods*. **1986**, *89* (2), 271-7.
28. Sadhasivam, L.; Durairaj, J., Evaluation profile of silver nanoparticle synthesized by Aloe vera extract. *Int. J. Chem. Tech. Res.* **2014**, *6*, 4379-4385.